Supplementary Information for

Core-shell-shell cytocompatible polymer dot-based particles with near-infrared emission and enhanced dispersion stability

Hannah R. Shanks[a], Mingning Zhu[a], Amir H. Milani[a], James Turton[a] ,Sarah Haigh[a], Nigel W. Hodson[b], Daman Adlam[c], Judith Hoyland[c, d], Tony Freemont[c, d] and Brian R. Saunders[a,]*

a) School of Materials, University of Manchester, MSS Tower, Manchester, M13 9PL, U.K.

b) BioAFM Facility, Faculty of Biology, Medicine and Health, Stopford Building, University of Manchester, Oxford Road, Manchester, M13 9PT, UK.

c) Division of Cell Matrix Biology and Regenerative Medicine, Faculty of Biology, Medicine and Health, University of Manchester, Oxford Road, Manchester, M13 9PT, U.K.

d) NIHR Manchester Musculoskeletal Biomedical Research Centre, Central Manchester Foundation Trust, Manchester Academic Health Science Centre, Manchester, UK

EXPERIMENTAL

Materials

Poly[2-methoxy-5-(2-ethylhexyloxy)-1,4-phenylenevinylene (MEH-PPV, M_n = 40,000 – 70,000 g/mol), silicon 2,3-naphthalocyanine bis(trihexylsilyloxide) (NIR775, 95 %), ammonium persulfate (APS, 98 %), ethyl acrylate (EA, ≥ 95 %), 1,4-butanediol diacrylate (BDDA, 90 %), and cumene terminated poly(styrene-*co*-maleic anhydride) (PSMA, M_n ~ 1,700 g/mol, 68 wt.% styrene) were all purchased from Sigma-Aldrich and used as received. THF (99.8 %) was purchased from Fisher Scientific UK Ltd and used as received. Methacrylic acid (MAA, (≥ 99 %) was purchased from VWR International Ltd and also used as received. All water used was ultra-high purity and was distilled and deionised. Alexa Fluor™ 430 NHS Ester (succinimidyl ester) was purchased from ThermoFisher Scientific and used as received.

Polymer dot synthesis

The method used to prepare our polymer dots (PDs) is a variation of the method reported by Wu et al.[1] A solution was prepared by dissolving PSMA (500 µg) in THF (5.0 mL) under an inert atmosphere at room temperature. A separate MEH-PPV solution was prepared in THF (170 mL with a concentration of 58.8 µg/mL), which was then combined with the PSMA solution. The concentrations of MEH-PPV and PSMA in the combined solution were 50 µg/mL and 10 µg/mL respectively. NIR775 was then dissolved in the combined solution at a concentration of 0.50 µg/mL. A portion of the MEH-PPV/NIR775/PSMA solution (50 mL) was quickly added to water (100 mL) with sonication. The sonication was continued for a further 10 min. Finally, the THF was removed by rotary evaporation at 30 ^{o}C. The PD dispersion was filtered through a 0.2 µm syringe filter before use.

Core-shell-shell polymer dot particle synthesis

Core-shell-shell (CSS) PD/PEA-MAA-BDDA/PD particles were prepared using seed-feed emulsion polymerisation using a starved feed of the comonomer solution. A sample of PD dispersion (45.0 mL) was prepared with a concentration of 25 μg/mL. APS initiator (1.0 mL of 1.0 mg/mL solution) was then added. The pH was decreased from 5.5 to 3.8 by addition of HCl (0.10 M). The dispersion temperature was then increased to 80 ^{o}C using an oil bath under an inert atmosphere. Separately, an aqueous comonomer solution (100 mL) containing a total of 0.23 g of EA (0.182 g, 1.82 mmol), MAA (0.046 g, 0.535 mmol) and BDDA (0.0023 g, 1.16 μmol) was prepared. An aliquot of the deoxygenated comonomer solution (2.5 mL) was fed via a syringe pump into the stirred PD dispersion over a period of 1 h. Once the monomer feed had finished, the polymerisation was allowed to continue for a further 5 h. The product was extensively dialysed using water.

Physical measurements

A Malvern Zetasizer NanoZS dynamic light scattering (DLS) instrument was used to measure the z-average diameter (d_z) and zeta potential data. These measurements were conducted at pH 5.5 unless otherwise stated. TEM images were obtained using a Tecnai 12 Biotwin, with a Gatan 1k CCD camera. Bright field imaging was used at 80 kV. Samples were prepared using ultra-thin lacey carbon and copper TEM grids (Agar Scientific) dried at room temperature. Scanning TEM imaging was performed on a probe side aberration corrected Titan ChemiSTEM with a convergence angle of 21 mrad, a 100 pA probe current and an accelerating voltage of 200 kV. Bright field and annular dark field (ADF) images were acquired with ADF inner and outer angles of 38 and 87 mrad respectively and a dwell time of 20 μs/pixel. SEM data were obtained using a Philips FEGSEM microscope. UV-vis spectroscopy measurements were obtained using a Hitachi U-1800 spectrophotometer. A

FLS980 spectrometer from Edinburgh Instruments was used to obtain photoluminescence (PL) data. The excitation wavelength used for these measurements was 470 nm. Quantum yield (QY) values were obtained via the comparison method[2] which used Rhodamine 6G as the QY standard (QY = 0.94). This analysis was performed using a/e-UV-Vis-IR Spectral Software 2.2 from FluorTools.com. AFM data were obtained using a Bruker Multimode 8 and a Nanoscope V controller. ScanAsystTM (Peak Force Tapping) mode was used in air. The sample was deposited on poly(L-lysine) coated mica. The images obtained were converted to 3D using the Bruker Nanoscope Analysis software (v1.5).

Cytotoxicity

Human nucleus pulposus cells were cultured in Dulbecco's modified Eagle's medium supplemented with antibiotic/antimycotic (Sigma-Aldrich, UK), Glutamax and 10% fetal bovine serum (Thermo Fisher Scientific, UK) within a humidified 5% CO_2 incubator at 37 °C. Cells were harvested by trypsinisation and seeded at a density of 3 x 10^4 cells per well onto 13 mm sterile glass coverslips in 24 well culture plates. After overnight incubation, the media was replenished and 20 μL of 1.2 x 10^4 μg/mL CSS particles were introduced to the NP cell cultures, with controls receiving an equal volume of phosphate buffered saline (PBS). Cells were cultured up to 8 d and live/dead assays (Thermo Fisher Scientific, UK) were performed at each time-point (n = 2) according to the manufacturer's instructions. Images were obtained with an Olympus BX51 fluorescence microscope and an EVOS XL Core cell imaging system.

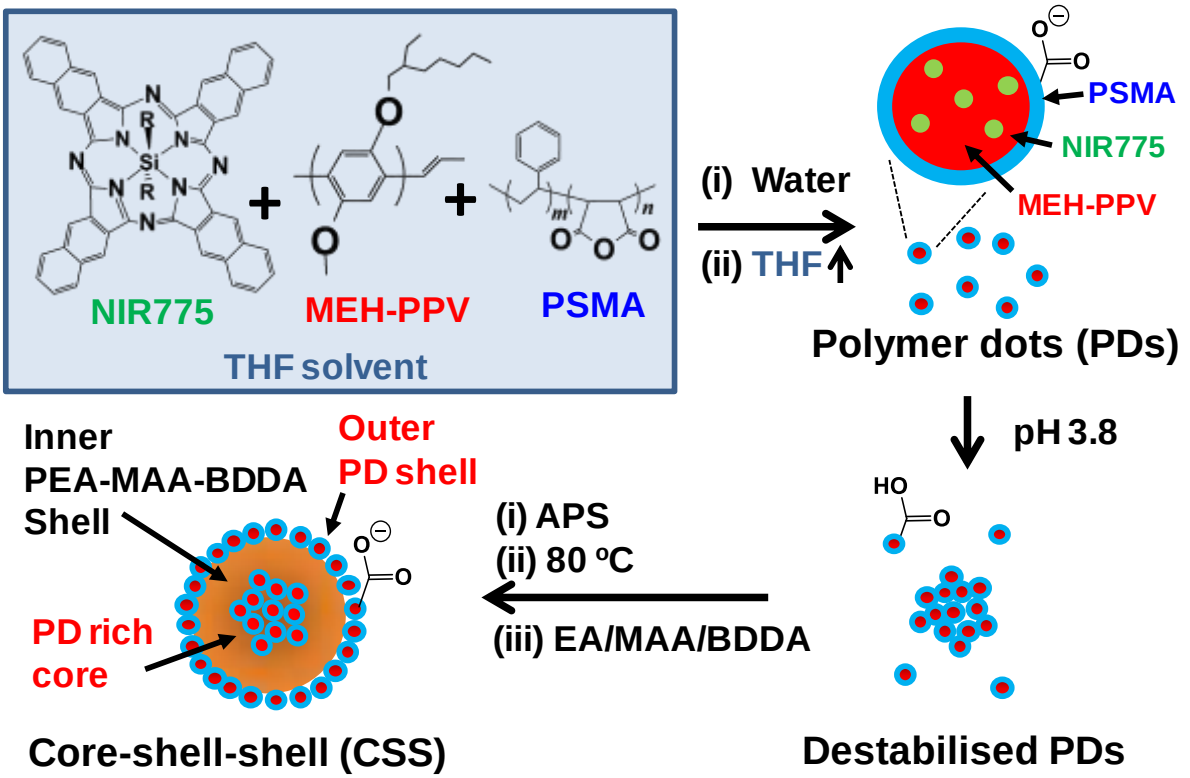

Scheme S1. Depiction of the method used to synthesise core-shell-shell (CSS) polymer dot (PD)-based particles. The PDs are prepared using nanoprecipitation and then destabilised by decreasing the pH and the acrylic shell grown. PD aggregates form in the core and additional PDs are adsorbed onto the outer shell.

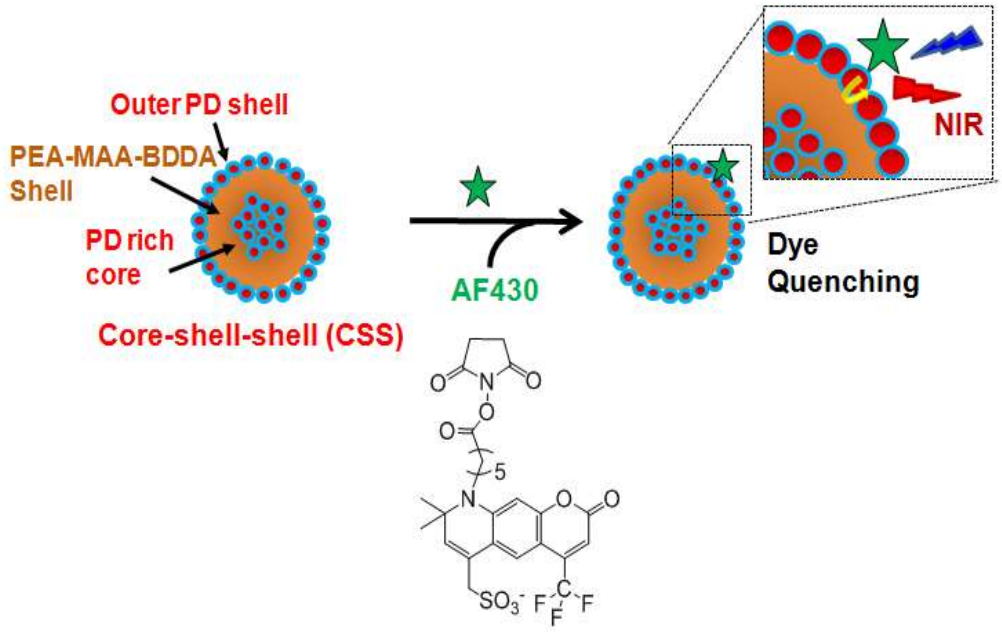

Scheme S2. Depiction of quenching of AF430 fluorescence via non-radiative resonance energy transfer (NRET).

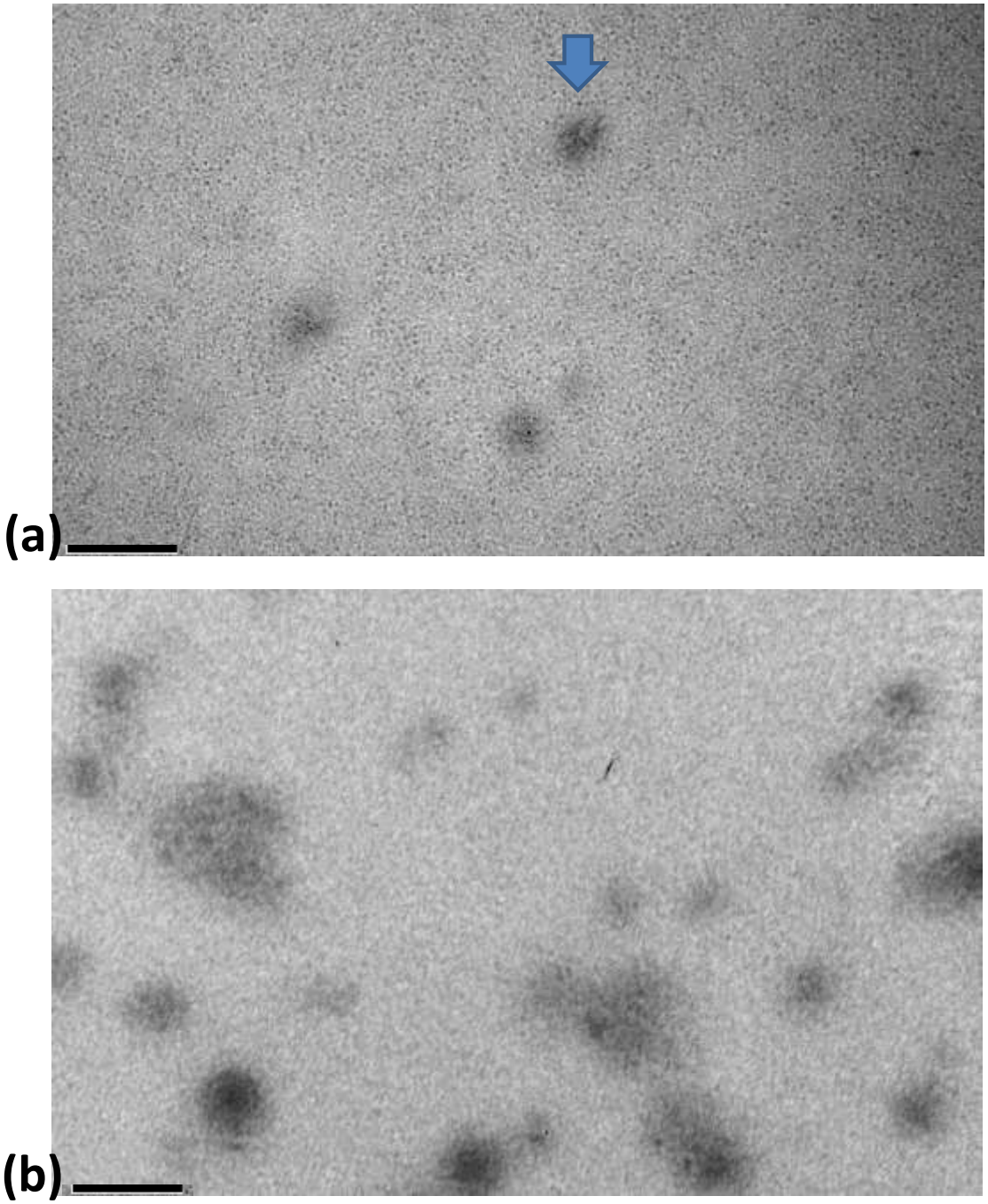

Figure S1. TEM images recorded for the PDs deposited from water at (a) pH 5.5 and (b) pH 3.8. Whilst the vast majority of the PDs were dispersed at pH 5.5 and appear as small dots in (a) occasional aggregates were present (arrow). However, decreasing the pH to 3.8 (b) resulted in most of the PDs forming small aggregates. The scale bars represent 100 nm.

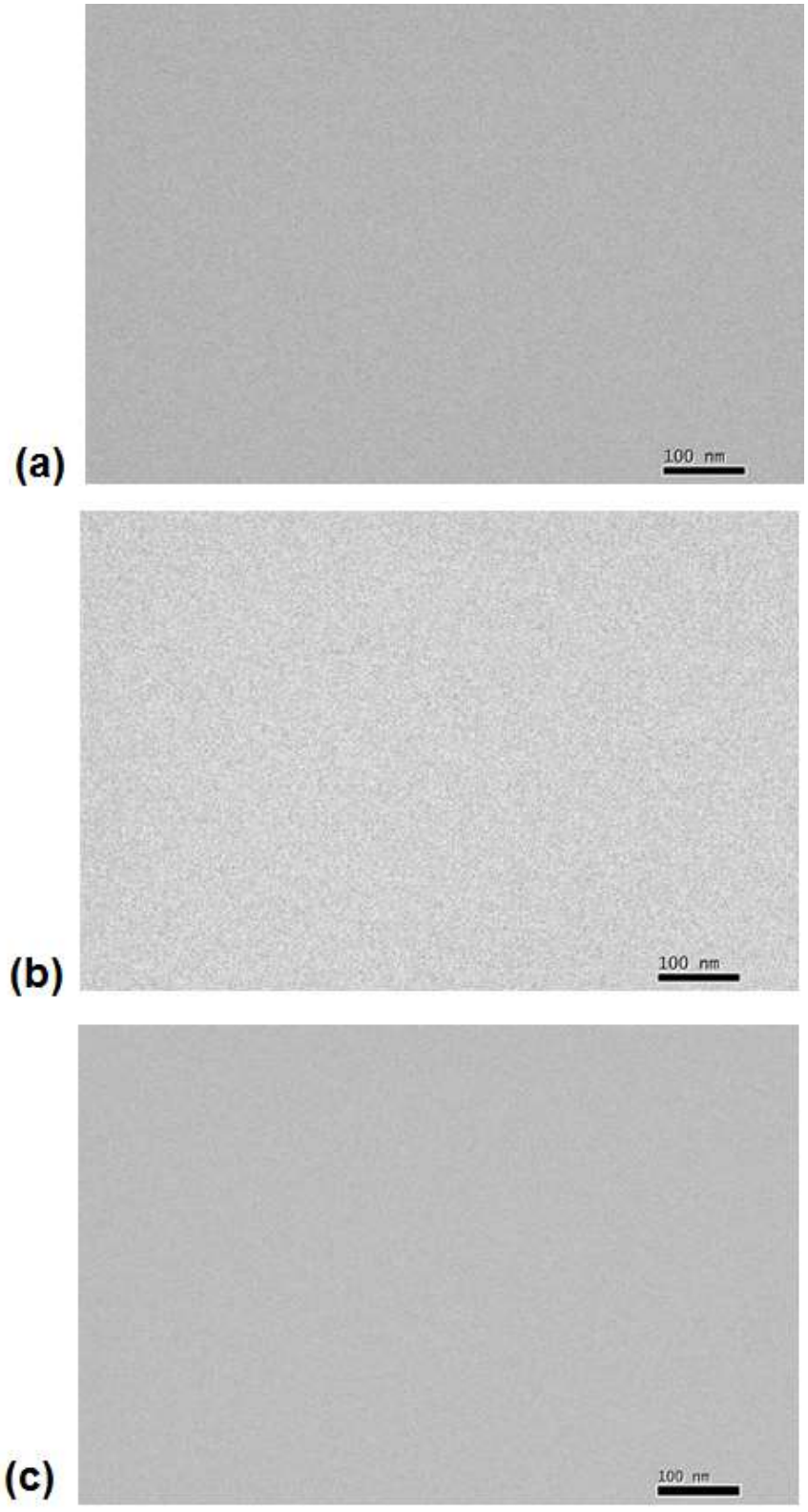

Figure S2. TEM images of (a) PSMA, (b) MEH-PPV, and (c) NIR775, deposited using the same method that was used to prepare the PD shown in Fig. S1(a). All three components were required to give PDs.

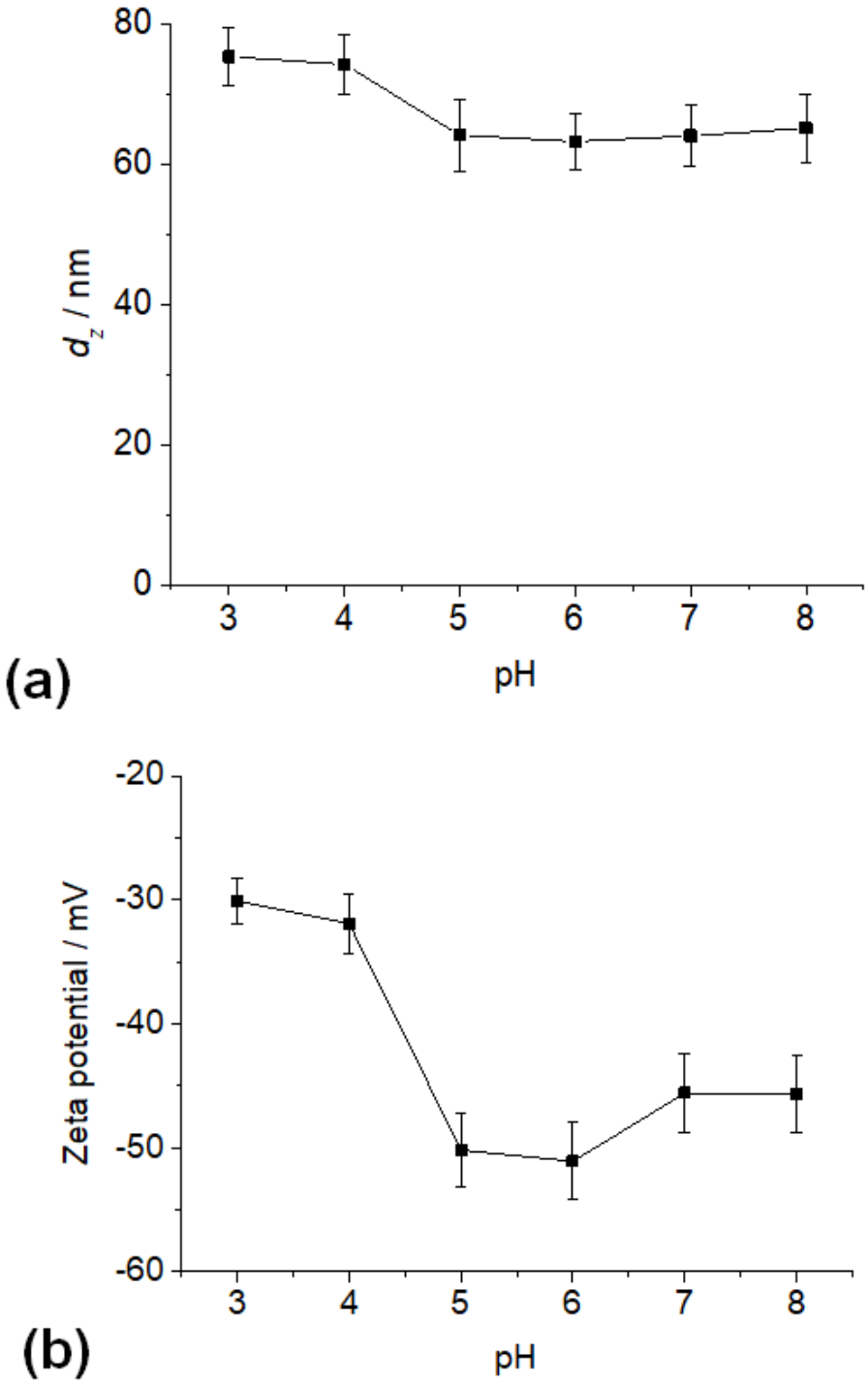

Figure S3. pH-dependent (a) z-average diameter (d_z) data and (b) zeta potential data measured for PD dispersions. The d_z data are obtained by dynamic light scattering (DLS) and is therefore dominated by the presence of occasional large PD aggregates (see Fig. S1a) so does not represent the size of the individual PDs.

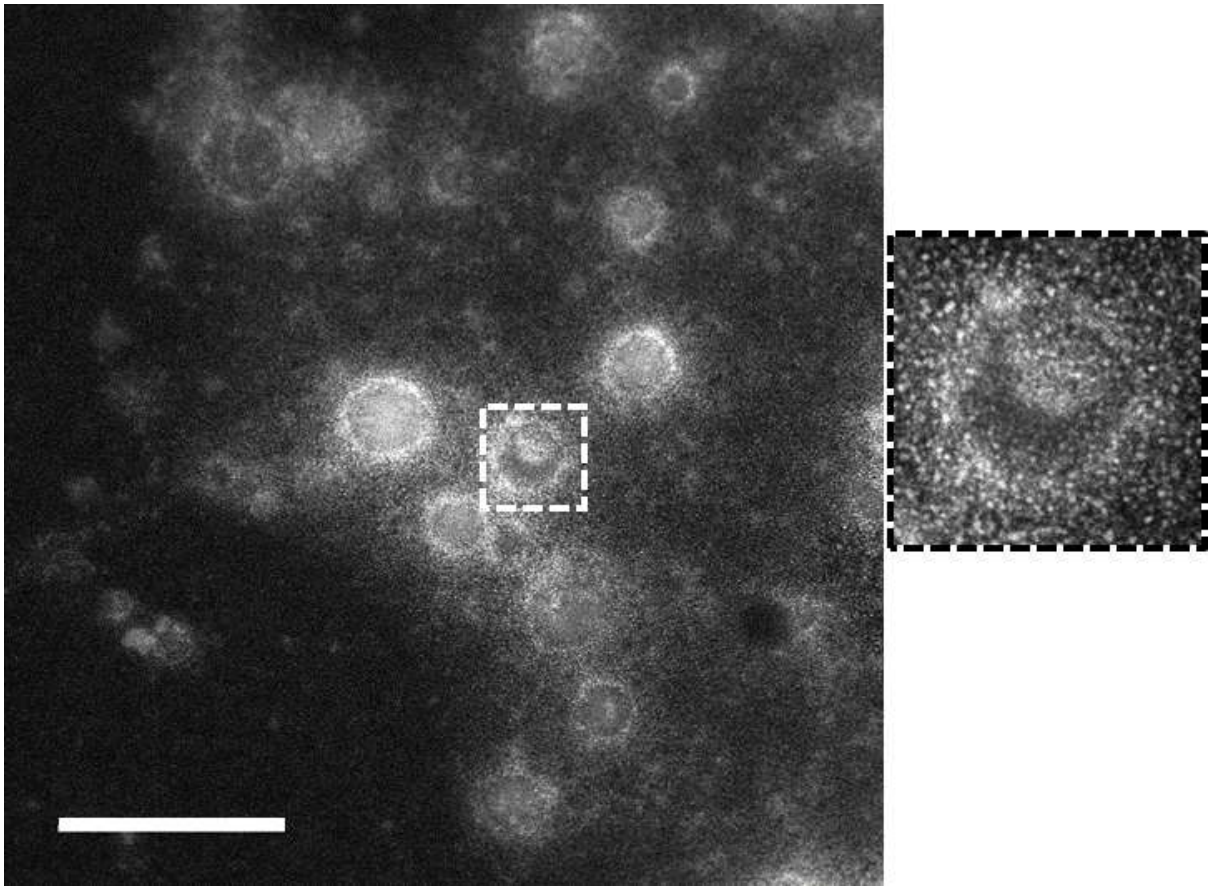

Figure S4. Dark field STEM image of CSS particles. Scale bar represents 200 nm. The inset is 100 nm x 100 nm. Note that for this technique the highest electron contrast species appear the brightest.

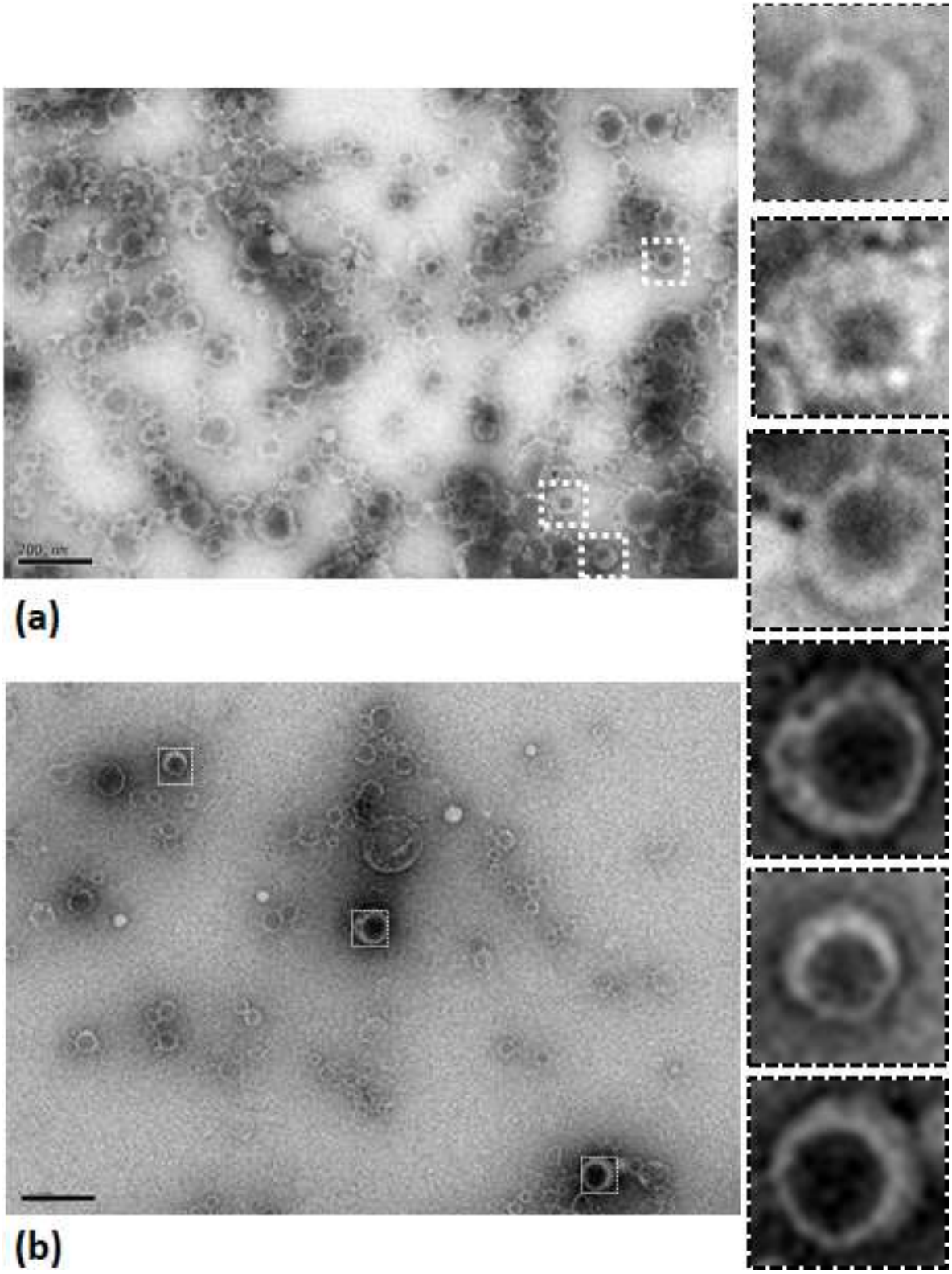

Figure S5. Lower magnification TEM images obtained for the CSS particles. Scale bars represent 200 nm. The insets are 100 nm x 100 nm.

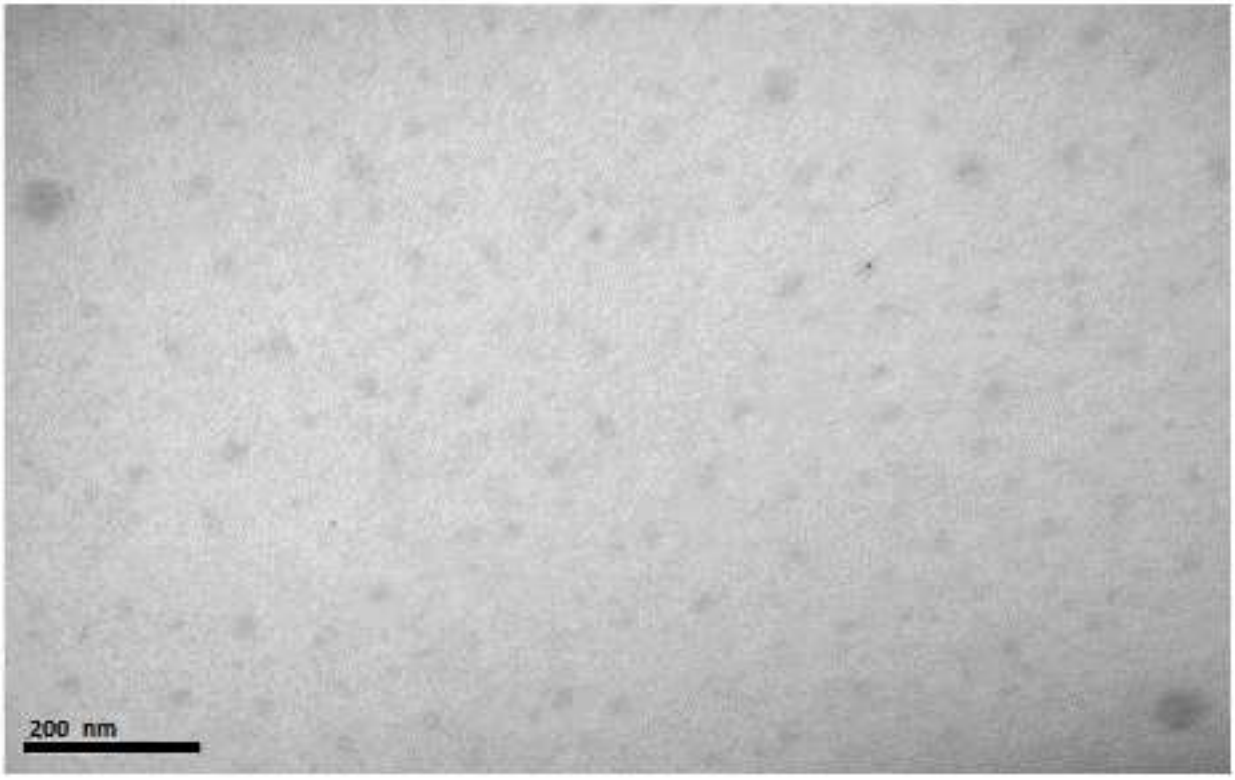

Figure S6. TEM image of PEA-MAA-BDDA particles with the same nominal composition as the inner shells of the CSS particles.

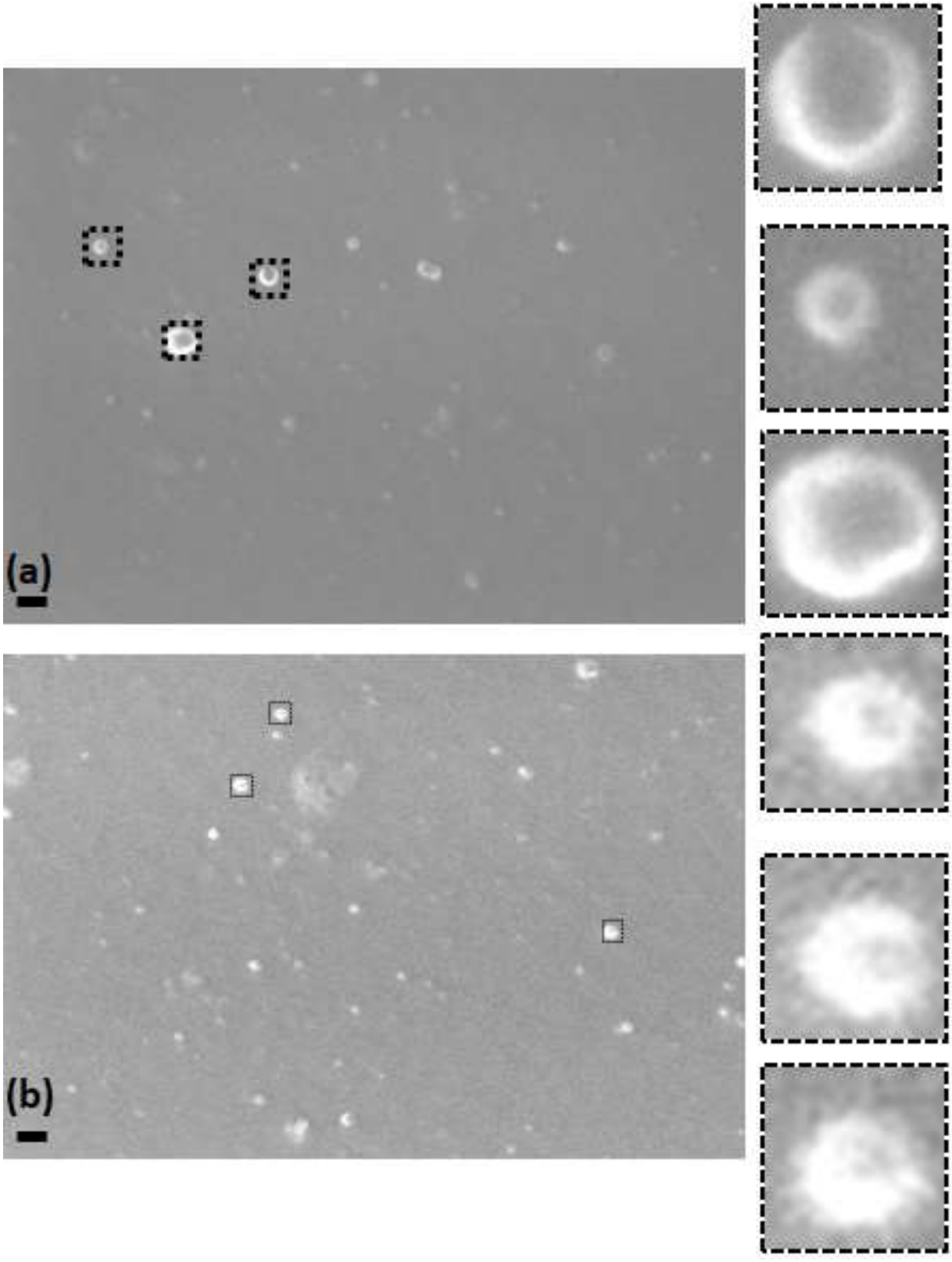

Figure S7. Representative SEM images obtained for the CSS particles. The scale bars represent 100 nm. The insets are 100 nm x 100 nm.

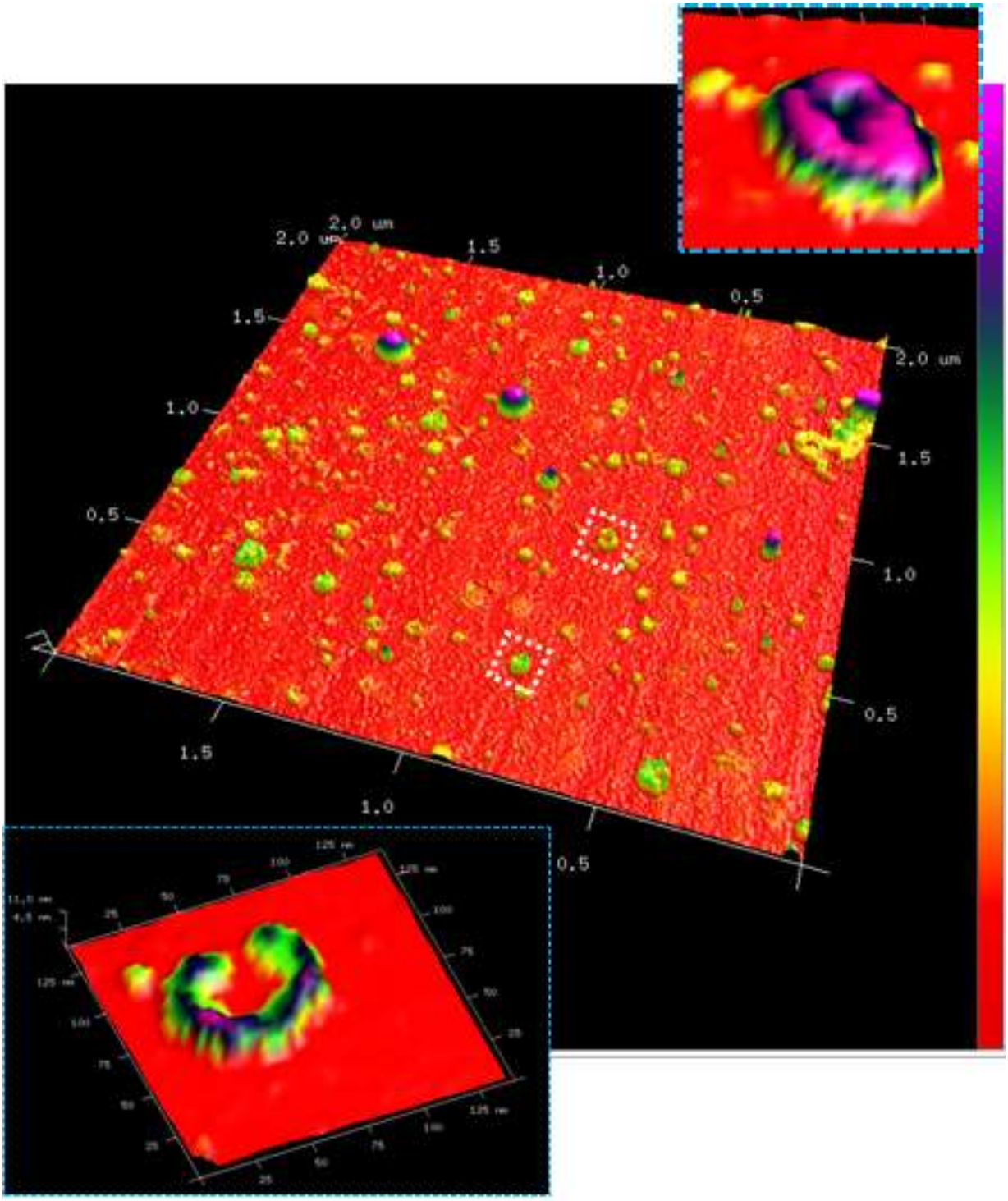

Figure S8. Lower resolution 3D AFM image of deposited CSS particles. The AFM measurements were performed in air.

Calculation of MEH-PPV extinction coefficient for the PDs

Several dispersions containing different weight percentages of PDs were prepared and UV-visible spectra measured. A calibration graph was constructed using the maximum MEH-PPV absorbance (500 nm) for each of the dispersions (see Fig. S9b). The absorbance values were corrected for scattering by subtracting a linear background. The extinction coefficient for MEH-PPV in the PDs dispersed in water was calculated as 0.209 $mL\mu g^{-1}cm^{-1}$. This value is comparable to a previously reported extinction coefficient, measured for MEH-PPV chains dissolved in chloroform[3] of 0.106 $mL\mu g^{-1}cm^{-1}$. The difference in these values may be due to the differences in the physical states and hence aggregation of MEH-PPV.

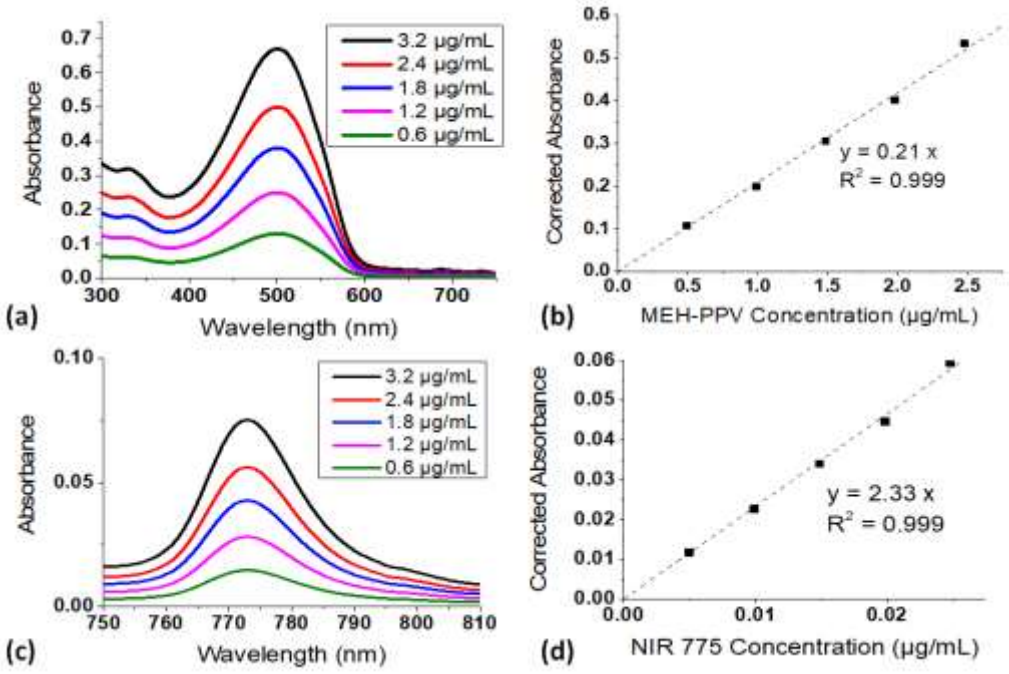

Figure S9. (a) Absorbance spectra with varying PD concentration. (b) Corrected absorbance for MEH-PPV measured at 500 nm as a function of PD concentration. (c) Spectra from (a) showing an enlargement of the NIR755 absorption maximum. (d) Corrected NIR775 absorbance measured at 773 nm as a function of the nominal NIR775 concentration.

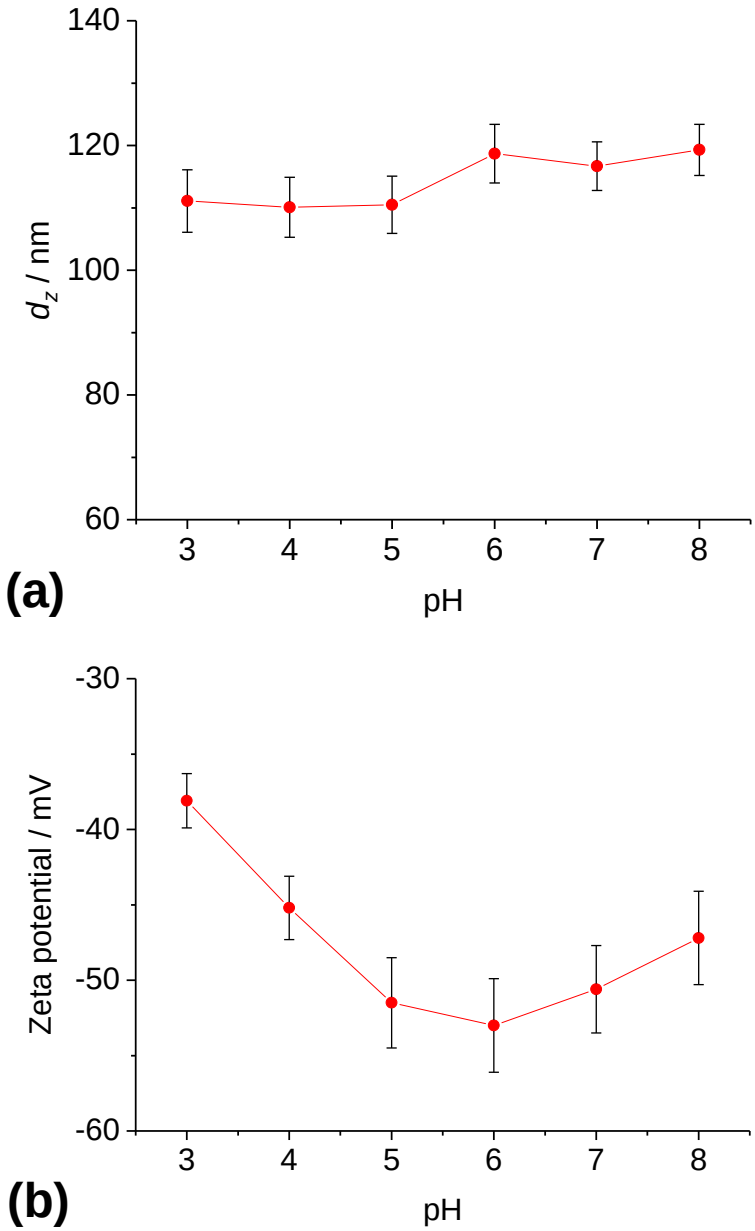

Figure S10. pH-dependent (a) z-average diameter (d_z) data and (b) zeta potential data measured for a CSS dispersion.

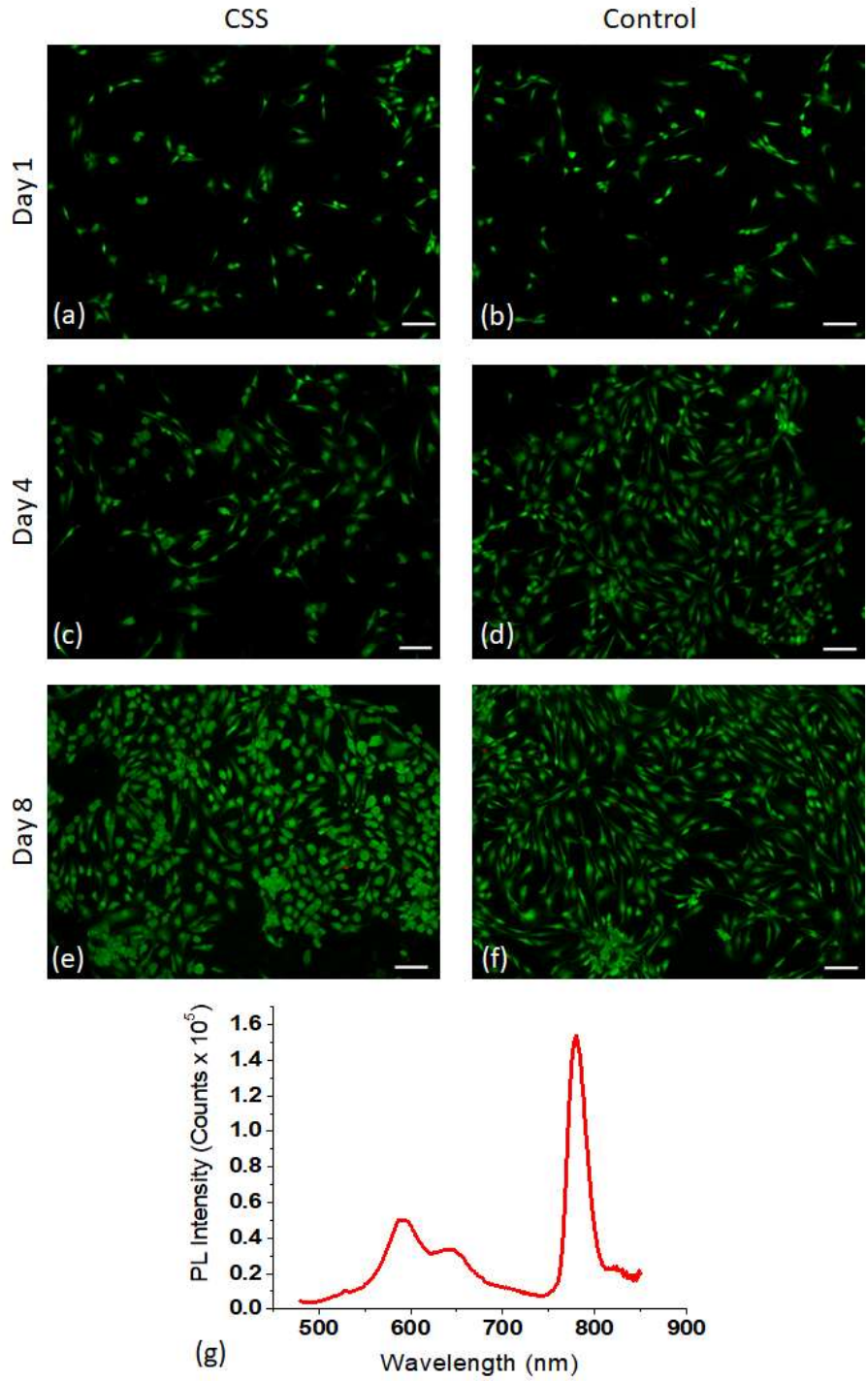

Figure S11. Live dead assays of nucleus pulposus cells in the presence of CSS particles (a, c and e) and a control without CSS particles (b, d and f) measured at different times. The scale bars represent 100 µm. Live cells are green and dead cells are red. (g) Photoluminescence (PL) emission spectrum of CSS particles at same concentration as used in the live dead assay.

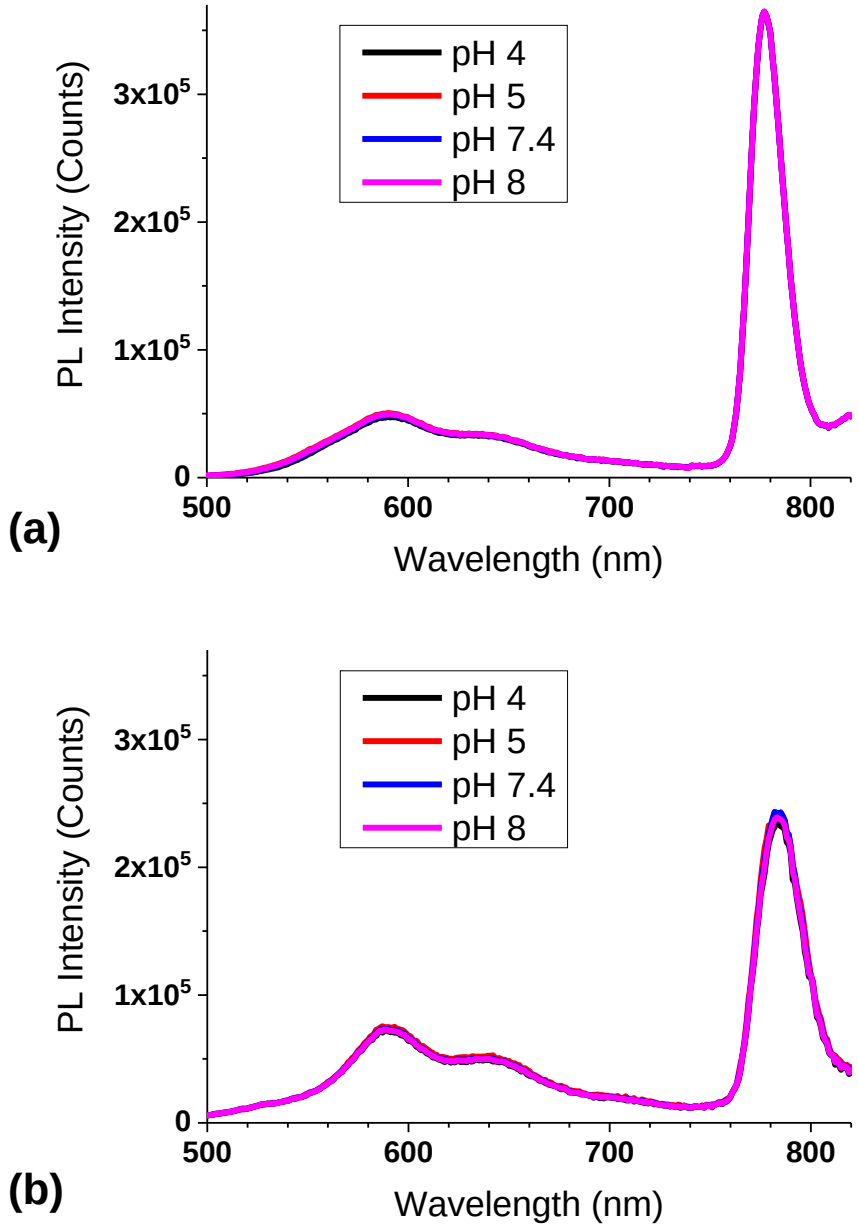

Figure S12. PL emission spectra for (a) PDs and (b) CSS particles measured at a variety of pH values. The spectra overlay and were not pH dependent in this range.

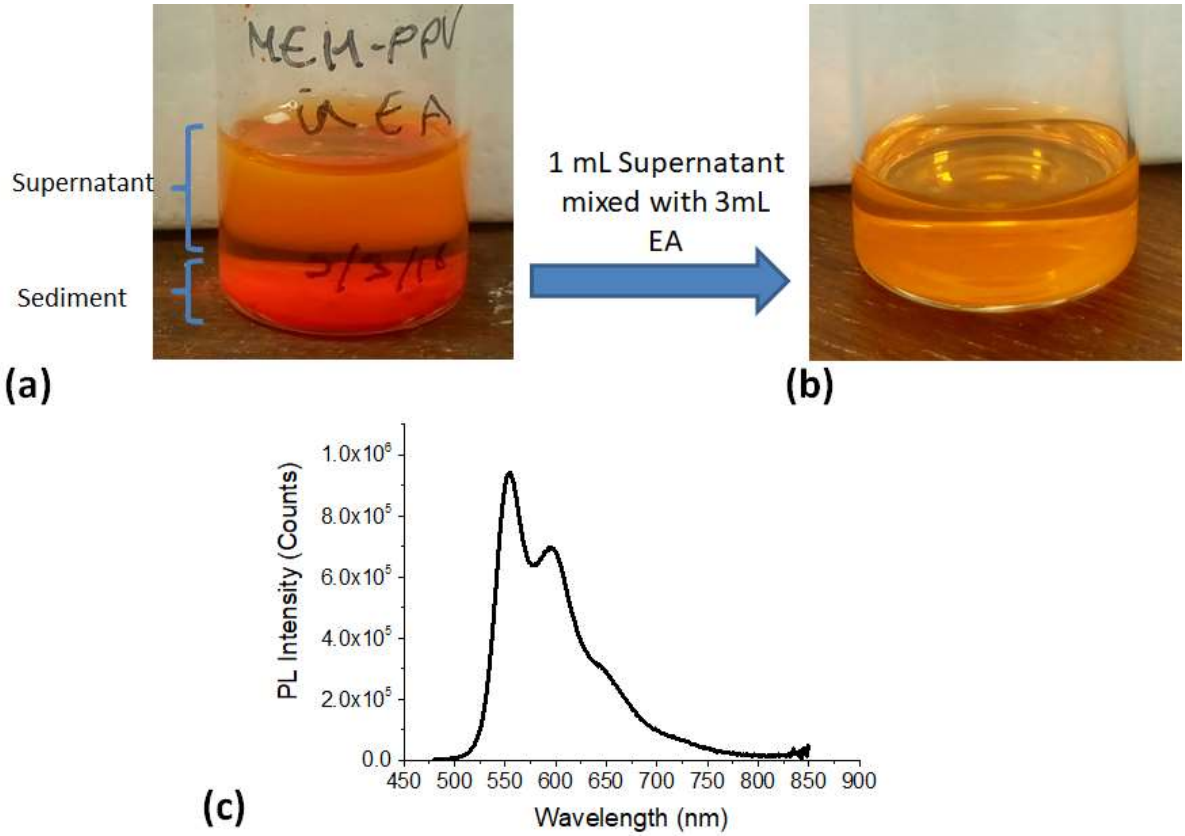

Figure S13. (a) Photograph showing MEH-PPV (5.3 mg) mixed EA (3.0 mL), after standing for 24 h. (b) Photograph of dispersion resulting from mixing 1.0 mL of supernatant from (a), with a further 3.0 mL of EA. (c) PL emission spectrum of the MEH-PPV solution in (b).

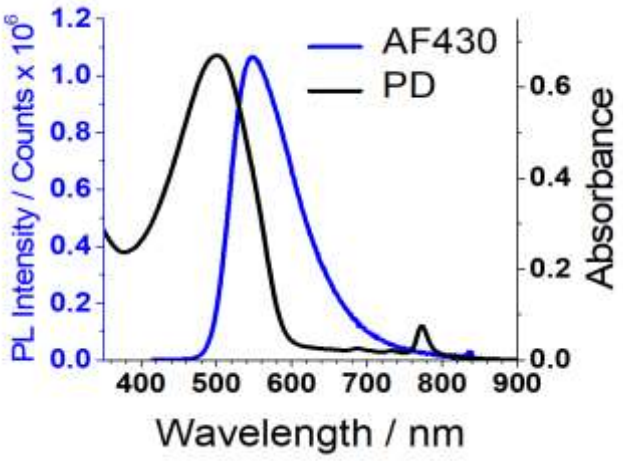

Figure S14. PL spectra for AF 430 dye dissolved in water (Blue). The UV-visible spectrum for dispersed PDs is also shown (Black).

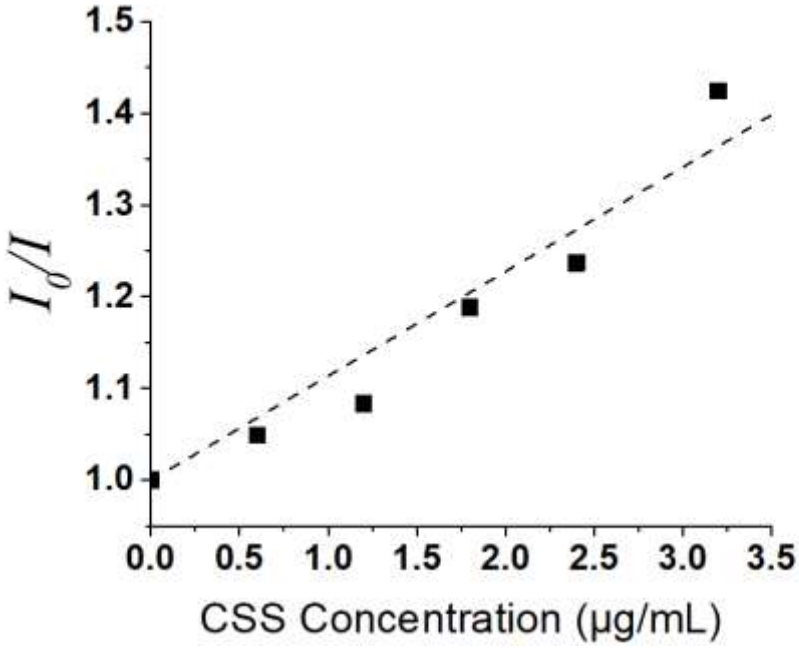

Figure S15. Variation of the PL intensity ratio for AF430 in the presence of different CSS concentrations. I_o and I are the PL intensities of the 547 nm peak (due to AF430) without or with added CSS particles according to the Stern-Volmer equation: $\frac{I_o}{I} = 1 + K_{sv}C_{CSS}$, where K_{sv} provides a measure of quenching[4]. The values for K_{sv} and R^2 from the fit were 0.114 mL/μg and 0.90, respectively.

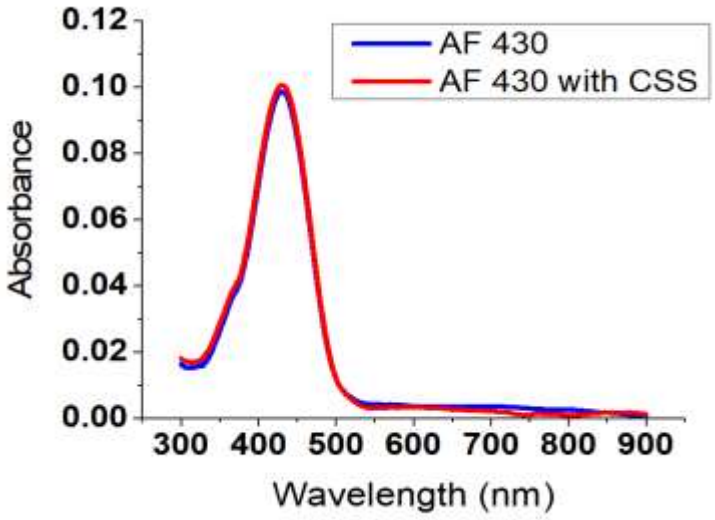

Figure S16. UV-visible spectra of AF 430 dye dispersion in water without (Blue) and with CSS (Red). For both samples, the concentration of AF 430 was 0.0047 mM.

Table S1. Quantum yields for CSS, PD and values for related systems from the literature.

System	**MEH-PPV**	**NIR775**	**Combined**	**Other**	**Reference**
CSS	0.11[a]	0.13[b]	0.24		This work
PD	0.07[a]	0.14[b]	0.21		This work
PD	0.03				5
PD	0.10				6
PD		0.07			7
PD		0.07			8
Ketoiminate-based polymer nanoparticles	-	-	-	0.07 – 0.39	9
NIR cyanovinylene PDs				0.21	10

[a] Wavelength range of 480 – 750 nm. [b] Wavelength range of 750 – 850 nm.

References

1. C. Wu, Y. Jin, T. Schneider, D. R. Burnham, P. B. Smith, and D. T. Chiu. *Angew. Chem., Int. Ed.* 2010, **49**, 9436-9440.
2. J. R. Lackowicz. *Principles of fluorescence spectroscopy, Springer, NY* 2006.
3. M. Zhang, L. Rene-Boisneuf, Y. Hu, K. Moozeh, Y. Hassan, G. Scholes, and M. A. Winnik. *J. Mater. Chem.* 2011, **21**, 9692-9701.
4. S. Verma, B. Tirumala Rao, A. K. Srivastava, H. S. Patel, S. Satapathy, M. P. Joshi, V. K. Sahu, and L. M. Kukreja. *J. Lumin.* 2014, **155**, 156-164.
5. S. N. Clafton, D. A. Beattie, A. Mierczynska-Vasilev, R. G. Acres, A. C. Morgan, and T. W. Kee. *Langmuir* 2010, **26**, 17785-17789.
6. C. Wu, C. Szymanski, and J. McNeill. *Langmuir* 2006, **22**, 2956-2960.
7. Y. Jin, F. Ye, M. Zeigler, C. Wu, and D. T. Chiu. *ACS Nano* 2011, **5**, 1468-1475.
8. D. Chen, I. C. Wu, Z. Liu, Y. Tang, H. Chen, J. Yu, C. Wu, and D. T. Chiu. *Chem. Sci.* 2017, **8**, 3390-3398.
9. C. Dai, D. Yang, X. Fu, Q. Chen, C. Zhu, Y. Cheng, and L. Wang. *Polym. Chem.* 2015, **6**, 5070-5076.
10. S. Kim, C.-K. Lim, J. Na, Y.-D. Lee, K. Kim, K. Choi, J. F. Leary, and I. C. Kwon. *Chem. Commun.* 2010, **46**, 1617-1619.